[13] R. N. Euwema and D. J. Stukel, Phys. Rev. B 1, 4692 (1970).

[14] For example, see L. J. Page and E. H. Hygh, Phys. Rev. 131, 3472 (1970); or A. B. Kunz, Phys. Rev. B 2, 5015 (1970).

[15] D. M. Roessler and W. C. Walker, J. Phys. Chem. Solids 28, 1507 (1967).

[16] K. E. Teegarden and D. B. Dutton, Phys. Rev. 155, 896 (1967).

[17] W. B. Fowler, Phys. Rev. 151, 657 (1966).

[18] R. C. Chaney, E. E. Lafon, and C. C. Lin, Phys. Rev. B 4, 2734 (1971).

[19] G. S. Painter, Int. J. Quantum Chem. (to be published).

[20] C. Gout, R. Frandon, and J. Sadaca, Phys. Letters 11, 656 (1969).

[21] S. W. Duckett and P. H. Metzger, Phys. Rev. 137, A953 (1965).

[22] R. Haensel, C. Kunz, T. Sasaki, and B. Sonntag, Phys. Rev. Letters 20, 1436 (1968).

[23] F. C. Brown, C. Gähwiller, H. Fujita, A. B. Kunz, W. Scheifley, and N. Carrera, Phys. Rev. B 2, 2126 (1970).

[24] For example, see D. M. Roessler and W. C. Walker, Phys. Rev. 166, 599 (1968); J. E. Eby, K. J. Teegarden, and D. B. Dutton, *ibid.* 116, 1099 (1959).

[25] C. Y. Fong and M. L. Cohen, Phys. Rev. Letters 21, 22 (1968); Phys. Rev. 185, 1168 (1969).

[26] C. Kittel, *Introduction to Solid State Physics* (Wiley, New York, 1971), p. 121.

[27] J. C. Phillips and J. A. Van Vechten, Phys. Rev. Letters 22, 705 (1969).

[28] A. G. Buntar and A. F. Margolina, Ukr. Fiz. Zh. 15, 359 (1970).

[29] T. Fukamachi and S. Hosoya, J. Phys. Soc. Japan 29, 736 (1970).

PHYSICAL REVIEW B VOLUME 6, NUMBER 10 15 NOVEMBER 1972

Effects of Domain Shapes on Second-Harmonic Scattering in Triglycine Sulfate

G. Dolino
Laboratoire de Spectrométrie Physique, Cédex 53 (38) *Grenoble-Gare, France*

(Received 30 March 1972)

A general description is given of the second-harmonic scattering of light by domains in a ferroelectric crystal. In addition to the usual second-harmonic beam, one observes second-harmonic light in new directions. The angular pattern of scattered light depends upon domain shapes. Plane parallel or cylindrical domains give very different diffraction diagrams. An experimental observation of this phenomenon in triglycine sulfate is given, where the variation of the second-harmonic intensity is correlated to changes in the domain structure. The anisotropy of the domains's cross sections leads to an anisotropic diffraction pattern.

I. INTRODUCTION

The phenomenon of second-harmonic generation (SHG) of light is observed when an intense light beam interacts with a noncentrosymmetric material.[1] If this material is inhomogeneous, second-harmonic scattering (SHS) is produced. This was observed for the first time in NH_4Cl by Freund[2] and then in triglycine sulfate (TGS).[3,4] The origin of this effect can be easily understood by considering the spatial modulation of nonlinear polarization by the domain structure. The effect of domains on the intensity of SHG was first observed by Miller on ferroelectric crystals of $BaTiO_3$.[5]

We have previously described the angular pattern of SHS which is observed on TGS crystals.[4] Here we give new theoretical and experimental results of the effects of domain shapes on SHS. The discussion is centered on ferroelectric materials, but some results can also be applied to the case of twins.

Section II is a general theoretical discussion of SHS where the effects of surface and domains are separated. Perfect correlation in one direction (cylindrical domains) or in two directions (plane parallel domains) leads to the characteristic scattering pattern. Particular attention is paid to the asymptotic behavior of the intensity for large scattering angles. In Sec. III new experimental results obtained at room temperature on TGS are presented. After recalling the main nonlinear optical properties of TGS we study the variation of intensity as a function of the scattering vector $\Delta\vec{k}$, the effect of the anisotropy of domain cross sections, and give some information on the effects of thermal treatments on domain structure and on SHS.

II. THEORY

A. Ferroelectricity and SHG

When a light beam with an electric field $\vec{E}_\omega$ of frequency ω is propagating in a crystal, it produces a linear polarization $\vec{P}_\omega = \overleftrightarrow{\epsilon} \cdot \vec{E}_\omega$ and also a nonlinear polarization $\vec{P}_{2\omega} = (\overleftrightarrow{d} \cdot \vec{E}_\omega) \cdot \vec{E}_\omega$ which is observable if the light beam is intense enough.[1] $\overleftrightarrow{\epsilon}$ is the linear susceptibility tensor and $\overleftrightarrow{d}$ the nonlinear susceptibility tensor. SHG can occur only in noncentrosymmetric crystals, which is the case in ferroelectrics.

In the phenomenological theory of ferroelectricity it is customary to suppose that the ferroelectric phase is not much different from the paraelectric one, and that all differences can be ascribed to the spontaneous polarization $\vec{P}_s$ which appears during the transition. Therefore, one can expand the tensors describing physical properties, in ascending powers of $\vec{P}_s$, using coefficients (of tensorial form) which are the same in both phases, and which are, to a first approximation, temperature independent. Thus, we obtain the following expressions for $\overleftrightarrow{\epsilon}$ and $\overleftrightarrow{d}$:

$$\begin{aligned} \overleftrightarrow{\epsilon} &= \overleftrightarrow{\epsilon}_0 + \overleftrightarrow{\epsilon}_1 \cdot \vec{P}_s + (\overleftrightarrow{\epsilon}_2 \cdot \vec{P}_s) \cdot \vec{P}_s \ , \\ \overleftrightarrow{d} &= \overleftrightarrow{d}_0 + \overleftrightarrow{d}_1 \cdot \vec{P}_s + (\overleftrightarrow{d}_2 \cdot \vec{P}_s) \cdot \vec{P}_s \ . \end{aligned} \tag{1}$$

As $\overleftrightarrow{\epsilon}$ is a second-order tensor, $\overleftrightarrow{\epsilon}_0$ is also second-order, $\overleftrightarrow{\epsilon}_1$ is third order, and so on. In the same way $\overleftrightarrow{d}$ and $\overleftrightarrow{d}_0$ are third order, $\overleftrightarrow{d}_1$ is fourth order, etc. All these tensors are the same in both phases, and so they reflect the symmetries of the most symmetrical phase, the paraelectric one. Now one can distinguish between ferroelectric crystals which are centrosymmetric and those which are noncentrosymmetric in the paraelectric phase. In the first case all the tensors in Eq. (1) can be different from zero. But in the second case, the centrosymmetric paraelectric phase, all tensors of odd orders are null. Then

$$\begin{aligned} \overleftrightarrow{\epsilon} &= \overleftrightarrow{\epsilon}_0 + (\overleftrightarrow{\epsilon}_2 \cdot \vec{P}_s) \cdot \vec{P}_s + \text{terms with even powers of } \vec{P}_s \ , \\ \overleftrightarrow{d} &= \overleftrightarrow{d}_1 \cdot \vec{P}_s + \text{terms with odd powers of } \vec{P}_s \ . \end{aligned} \tag{2}$$

Then, in the paraelectric phase, there is no SHG arising from dipolar effects. In the following we consider only ferroelectric crystals with a centrosymmetric paraelectric phase, which have only 180° domains. (The spontaneous polarization is always parallel to the same direction, only its sense changes.) The susceptibility tensors (and so the refractive indices) are the same in domains of positive or negative polarizations. If domain walls have no effects, the refractive indices are the same throughout the crystal and so one cannot observe the domain structure by ordinary optical means. But for SHG, the nonlinear susceptibility is to a first approximation proportional to $\vec{P}_s$ (the sign of which changes from one domain to the other). This modulation of the nonlinear polarization produces SHS as is explained below.

B. General Formulation of SHS

We shall study the problem of SHS in a nonlinear crystal, with homogeneous linear properties and with only 180° domains. This crystal is surrounded by a linear medium with the same optical properties as the crystal to suppress the reflections on surfaces. The coefficients of the nonlinear susceptibility tensor of the crystal are taken to be proportional to the magnitude of the spontaneous polarization at the point $\vec{r}$, $P(\vec{r}) = \pm |\vec{P}_s|$. We suppose that the second-harmonic (SH) intensity is small, so that the intensity of the fundamental is not depleted. In this parametric approximation one can calculate the SH intensity by two methods: Fourier transform in plane waves,[4] or Green's functions, which was used previously for SHG by focused beams.[6,7] Here we use the latter method.

First we calculate the electric field $\vec{E}_{2\omega}$ radiated at a point r' by a volume of nonlinear material, small relative to the wavelength of light situated at a point r. For an isotropic medium, it is given by[6]

$$\vec{E}_{2\omega}(\vec{r}\,') = \left(\frac{2\omega}{c}\right)^2 (\overleftrightarrow{I} - \vec{s}\vec{s}) \cdot \vec{P}_{2\omega}(\vec{r})\, e^{i2\vec{k}_1\cdot\vec{r}} \times \frac{1}{|\vec{r} - \vec{r}\,'|}\, e^{i\vec{k}_2\cdot(\vec{r}\,'-\vec{r})} \ . \tag{3}$$

$\vec{k}_1$ and $\vec{k}_2$ are the wave vectors of the fundamental and SH waves. $\overleftrightarrow{I} - \vec{s}\vec{s}$ is a projection operator used to select the transverse component of $\vec{P}_{2\omega}$ with $\overleftrightarrow{I}$ the second-order unity tensor and $\vec{s}$ the unitary vector along $\vec{k}_2$. When considering a macroscopic body it is necessary to integrate (3) over the entire volume of the sample. For a point at a large distance R from the sample one gets, with $\vec{P}_{2\omega} = \overleftrightarrow{d}_1 \cdot \vec{u} P(\vec{r}) \vec{E}_\omega \vec{E}_\omega$ (where $\vec{u}$ is a unit vector along the polar axis),

$$\vec{E}_{2\omega}(R) = \left(\frac{2\omega}{c}\right)^2 (\overleftrightarrow{I} - \vec{s}\vec{s}) \cdot (\overleftrightarrow{d}_1 \cdot \vec{u} \vec{E}_\omega \vec{E}_\omega) \times \frac{e^{i\vec{k}_2\cdot\vec{R}}}{R} F(\Delta\vec{k}) \ , \tag{4}$$

$$F(\Delta\vec{k}) = \int_v P(\vec{r})\, e^{i\Delta\vec{k}\cdot\vec{r}} d^3 r \ , \tag{5}$$

with $\Delta\vec{k} = 2\vec{k}_1 - \vec{k}_2$.

The intensity $I_{2\omega}$ in the direction $\vec{k}_2$ is given at a large distance from the sample by

$$I_{2\omega} \sim E_{2\omega} E^*_{2\omega} \sim |F(\Delta\vec{k})|^2 \ . \tag{6}$$

The SH intensity produced by the crystal is proportional to the square of the modulus of the Fourier transform of the polarization. For linear scattering, the analogous result is true only if multiple scattering can be neglected. For SHS this result is valid in the parametric approximation.

A formula such as (6) is also found for the intensity of small-angle x-ray scattering, where the polarization $P(\vec{r})$ is replaced by the electronic density $\rho(\vec{r})$.[8] Many results of this well-studied phenomenon can be used for SHS. The main difference is in the order of magnitude of the scattering vector. For x rays, $1/|\Delta\vec{k}|$ is of the order of 10–500 Å, for light it is between 1 and 1000 μ. In the case of media with anisotropic optical properties calculations are more complex, but the expression for the Green's function at a large distance from the sample has the same spatial variation as for an isotropic material[7] and so one also gets the same equation (6) for the scattered intensity at infinity. The principal difference between an anisotropic and an isotropic material is the existence, in the former, of waves with well-defined linear polarization (ordinary and extraordinary beams in an uniaxial crystal) which leads to the realization of phase matching[1] between beams of different polarizations. Depending upon the polarization of incident light, three nonlinear polarization waves with the different wave vectors can propagate in the crystal, each one giving rise to two scattered waves of orthogonal polarization.[4] In the following we consider only one nonlinear polarization wave giving rise to one well-defined scattered wave. So there is only one kind of scattering vector $\Delta\vec{k}$, the extremity of which lies on well-defined index surfaces.

We are going to show that there are two contributions to the SH intensity which can be separated by a suitable cut of the sample: One comes from the domain structure inside the crystal and can be called the heterogeneous part, while the other comes from the continuity conditions at the crystal surface and can be called the homogeneous part. We introduce a form factor of the crystal, $B(\vec{r}) = 1$, if $\vec{r}$ is inside the crystal, and $B(\vec{r}) = 0$, if it is outside. For a plane-parallel slab of thickness l, perpendicular to the z axis,

$$B(\vec{r}) = Y(z + \tfrac{1}{2}l) - Y(z - \tfrac{1}{2}l) \quad , \tag{7}$$

where $Y(z) = 0$ if $z < 0$ and $Y(z) = 1$ if $z > 0$. (The origin of the z axis is taken at the middle of the slab.) We can suppose that $P(\vec{r})$ is defined in all space so that

$$F(\Delta\vec{k}) = \int_{\text{all space}} P(\vec{r})\, B(\vec{r})\, e^{i\Delta\vec{k}\cdot\vec{r}}\, d^3r \tag{8}$$

$$= (2\pi)^{-3} \int P(\vec{q}) B(\Delta\vec{k} - \vec{q})\, d^3q \quad , \tag{9}$$

where $P(\vec{q})$ and $B(\vec{q})$ are the Fourier transforms of $P(\vec{r})$ and $B(\vec{r})$. The $(2\pi)^{-3}$ factor in the convolution product of Eq. (9) comes from the choice of the argument of the Fourier transform, so that[9]

$$\int e^{i\vec{k}\cdot\vec{r}} d^3r = (2\pi)^3\, \delta(\vec{k}) \quad , \tag{10}$$

where $\delta(\vec{k})$ is the Dirac distribution. If the Fourier transform of the domain structure is known, one can calculate the SH intensity directly. One can also use a correlation function to do this:

$$\begin{aligned} I_{2\omega} \sim |F(\Delta\vec{k})|^2 &= \int\int P(\vec{r})B(\vec{r})P(\vec{r}\,')B(\vec{r}\,') \\ &\quad \times e^{i\Delta\vec{k}\cdot(\vec{r}-\vec{r}\,')}\, d^3r\, d^3r' \\ &= \int d^3u\, e^{i\Delta\vec{k}\cdot\vec{u}} \int d^3r\, P(\vec{r}) \\ &\quad \times P(\vec{r}+\vec{u})B(\vec{r})B(\vec{r}+\vec{u}) \quad , \end{aligned} \tag{11}$$

with $\vec{u} = \vec{r} - \vec{r}\,'$.

In general the domain structure is not exactly known and it is necessary to make some assumptions to get the correlation function. If the domains are small enough, so that there is a great number of them in the light beam, one can suppose that the intensity produced by a large number of samples will be nearly the same, and can be given by some statistical mean value on a domain ensemble. We assume that

$$P(\vec{r})\, P(r + \vec{u}) = \langle P(\vec{r})\, P(\vec{r}+\vec{u})\rangle_{\text{av}} = C(\vec{u}) \quad , \tag{12}$$

where $\langle\rangle_{\text{av}}$ denotes an ensemble average. In general this average can be obtained by an integration in the plane perpendicular to the z axis where $B(\vec{r})$ is constant. We suppose that the correlation function $C(\vec{u})$ is independent of $\vec{r}$. In doing so we lost the interference effects which can arise between the domain structure and sample surfaces. Then

$$|F(\Delta\vec{k})|^2 = \int d^3u\, C(\vec{u})\, e^{i\Delta\vec{k}\cdot\vec{u}} \int d^3r\, B(\vec{r})B(\vec{r}+\vec{u}) \quad . \tag{13}$$

The second integral is then the autocorrelation function $S(\vec{u})$ of the shape of the crystal,

$$S(\vec{u}) = \int B(\vec{r})B(\vec{r}+\vec{u})\, d^3r \quad . \tag{14}$$

If $C(\vec{q})$ and $S(\vec{q})$ are the Fourier transforms of $C(\vec{u})$ and $S(\vec{u})$,

$$|F(\Delta\vec{k})|^2 = (2\pi)^{-3} \int C(\vec{q}) S(\Delta\vec{k} - \vec{q})\, d^3q \quad . \tag{15}$$

For a plane-parallel slab defined by Eq. (7) one obtains (by surface unit)

$$\begin{aligned} S(\vec{u}) &= |l - u_z| \quad \text{for } u_z \text{ inside } |-l, +l| \\ &= 0 \qquad\quad\ \ \text{for } u_z \text{ outside } |-l, +l| \quad , \end{aligned} \tag{16}$$

$$S(\vec{q}) = (2\pi)^2\, \delta(q_x)\, \delta(q_y) \left(\frac{2\sin\frac{1}{2}q_z l}{q_z}\right)^2 , \tag{17}$$

which is the usual result for the intensity of the SH intensity produced by a nonlinear slab.[1] If l is great enough (relative to the coherence length $l_c = \pi/|\Delta\vec{k}|$), $S(q_z)$ has a narrow peak around $q_z = 0$ and can be replaced by a Dirac distribution

$$\left(\frac{2\sin\frac{1}{2}q_z l}{q_z}\right)^2 = 2\pi l\, \delta(q_z) \tag{18}$$

because

$$\int_{-\infty}^{+\infty} \left(\frac{2\sin\frac{1}{2}q_z l}{q_z}\right)^2 dq_z = 2\pi l \quad .$$

With this approximation,

$$S(\vec{q}) = (2\pi)^3\, l\, \delta(\vec{q}) \quad . \tag{19}$$

In general, the correlation function $C(\vec{u})$ contains singular parts. If the mean value of the spontaneous polarization is not zero,

$$P_0 = (1/V) \int_v P(r)\, d^3r \neq 0 \quad ,$$

there is a singularity in the form of the δ distribution in the Fourier transform of $P(\vec{r})$ and also of $C(\vec{u})$,

$$C(\vec{q}) = (2\pi)^3 P_0^2 \delta(\vec{q}) + C'(\vec{q}) \ , \tag{20}$$

where $C'(\vec{q})$ is a regular function. [If the domain structure was very regular such as to form a true grating of reciprocal vector $\vec{q}_0$ there would be terms of the form $\delta(\vec{q} - n\vec{q}_0)$, where n is an integer; such a term, rather improbable in a real crystal, can be treated in the same manner as $\delta(\vec{q})$.] Then

$$|F(\Delta\vec{k})|^2 = P_0^2 S(\Delta\vec{k}) + (2\pi)^{-3} \int C'(q) S(\Delta\vec{k} - \vec{q}) d^3q \ . \tag{21}$$

As $C'(q)$ is a regular function which is supposed to have a smooth variation, one can use the approximate form of Eq. (19) for the second term:

$$|F(\Delta\vec{k})|^2 = (2\pi)^2 P_0^2 \delta(\Delta k_x)\delta(\Delta k_y) \left(\frac{2\sin\frac{1}{2}\Delta k_z l}{\Delta k_z}\right)^2 + l\, C'(\vec{q}) \ . \tag{22}$$

Consequently, there are two parts in the intensity: The first term is the same as for a homogeneous slab of uniform polarization P_0. The second term arises from the domain structure and gives a diffuse scattering. If one measures the intensity in all of the reciprocal space, one can get the domain correlation function by the inverse Fourier transform. The scattered intensity can be calculated in considering only domains of one sign. We take

$$P(\vec{r}) = P_s[1 - 2\eta(\vec{r})] \ , \tag{23}$$

with $\eta(\vec{r}) = 0$ for $\vec{r}$ inside a positive domain, $\eta(\vec{r}) = 1$ for $\vec{r}$ inside a negative domain:

$$\begin{aligned} C(\vec{u}) &= P_s^2 \langle [1 - 2\eta(\vec{r})][1 - 2\eta(\vec{r} + \vec{u})] \rangle_{\text{av}} \\ &= 2P_0P_s - P_s^2 + 4P_s^2 \langle \eta(\vec{r})\eta(\vec{r} + \vec{u}) \rangle_{\text{av}} \ , \end{aligned} \tag{24}$$

with

$$P_0 = \langle P(\vec{r}) \rangle_{\text{av}} = P_s[1 - \langle 2\eta(r) \rangle_{\text{av}}] \ .$$

Now we shall discuss the particular form of the intensity pattern obtained when there is perfect correlation in one or two dimensions. Perfect correlation in one dimension in a ferroelectric is often found in order to obey the condition $\text{div}\vec{P} = 0$ in the bulk which leads to cylindrical walls parallel to the polar axis.[10] Furthermore, to reduce the elastic deformation energy, domain walls are often parallel to some crystallographic direction[10] and then the polarization depends only on a one-dimensional coordinate.[10]

C. One-Dimensional Models

In this case the polarization is a function of only one variable, and this leads to the existence of plane-parallel domains. The effect of such a domain structure on SHG was first observed by Miller[5] on $BaTiO_3$ and then by Vogt *et al.* on $NaNO_2$.[11] They give a result for the intensity in two limiting cases of near phase matching or of perfect disorder. Freund observed the SHS from an irregular plane-parallel domain structure in NH_4Cl.[2] The correlation function for such a domain structure is of the form

$$C(\vec{q}) = \delta(q_x')\delta(q_y') C(q_z') \ , \tag{25}$$

where we have made the choice of a new reference frame $0X'Y'Z'$, with $0Z'$ perpendicular to domain walls. As before, if the mean polarization is not zero, there is a $\delta(q_z')$ distribution to $C(\vec{q})$. In this case the intensity is given by Eq. (22). If the crystal surface is not parallel to the domain walls there are two peaks in two different angular directions: One comes from the homogeneous contribution with a scattering vector $\Delta\vec{k}$ perpendicular to the surface, and shows the oscillations of $|(\sin\frac{1}{2}\Delta k l)/\Delta k|^2$ and has a maximum in the phase-matching direction $\Delta k = 0$. The other, the inhomogeneous contribution, has a scattering vector perpendicular to domain walls and has a maximum when $l_c = \pi/|\Delta\vec{k}|$ is of the order of the domain width. This maximum is well marked if the domains form a regular lattice. If the surface is parallel to domain walls there is only one peak and the homogeneous and inhomogeneous contributions are mixed together. In this case, with N domain walls at point z_j, and the surface at $z = 0$ and $z = l$, and supposing that the first domain is positive, one has[5]

$$F(\Delta k) = \frac{P_s}{i\Delta k} [-1 + 2e^{i\Delta k z_1} - 2e^{i\Delta k z_2} + \cdots + 2(-1)^{N-1} e^{i\Delta k z_N} + (-1)^N e^{i\Delta k l}] \ . \tag{26}$$

In the expression of the intensity there are terms of the form $e^{i\Delta k(z_j - z_{j'})}$. If there is no correlation between the domain walls the mean value of these terms for great Δk and for $j \neq j'$ is zero. Thus only the terms with the same indices contribute to the intensity so that

$$I \sim \frac{P_s^2}{(\Delta k)^2} \{|[-1 + (-1)^N e^{i\Delta k l}]|^2 + 4N\} \ . \tag{27}$$

For large Δk, there is a great increase of intensity by a factor of the order of N (the number of domain walls) and the asymptotic dependence is in Δk^{-2}. For an anisotropic crystal with a phase-matching direction it is possible, by rotating the crystal, to vary Δk from 0 to a finite value, and so to obtain the dependence of intensity on Δk. The exact variation for small Δk depends upon the correlation effects between domains, which are very important in one dimension and cannot be calculated in general cases. One must make a specific hypothesis as to the domain structure to go further. One of the simplest is to suppose that the wall positions are obtained by a Poisson procedure: The probability of finding a domain wall between z and $z+dz$ is $\lambda\, dz$. The Fourier transform of the correlation function is then equal to[12]

$$C(\Delta k) = 4\lambda/(4\lambda^2 + \Delta k^2) \quad . \tag{28}$$

If only the distribution of domain widths is known, one cannot calculate interference effects between domains, and it is necessary to suppose that there is no correlation between domains,[11] which is a suitable approximation only when there are few small domains.

D. Two-Dimensional Models

Now the polarization depends only on two variables X', Y' and the domains are cylinders parallel to the $0Z'$ direction. The Fourier transform of the correlation function depends also upon two variables, and Eq. (22) gives

$$|F(\Delta\vec{k})|^2 = (2\pi)^2 P_0^2\, \delta(q_x)\delta(k_y)\, \frac{2\sin\frac{1}{2}\Delta k_z l}{\Delta k_z} + 2\pi l C(\Delta k_{X'}, \Delta k_{Y'})\delta(\Delta k_{Z'}) \; , \tag{29}$$

with $0Z$ always perpendicular to the crystal surfaces. The first term gives a peak for $\Delta\vec{k}$ perpendicular to the surface. But now the second term gives a scattered line for $\Delta\vec{k}$ perpendicular to the domain axis (which was indeed observed on TGS [4]; see also Sec. III). In the following we will calculate the scattered intensity for a few simple cases.

We consider first the case of cylinders with a circular cross section of radius a. Following Eq. (24), we only calculate the Fourier transform of the cylinders, supposed to be, for example, positive domains. Then

$$f(\Delta\vec{k}) = \int_{\text{cylinders}} e^{i\Delta\vec{k}\cdot\vec{r}}\, d^3r = 4\pi^2 a^2 [J_1(m)/m]\,\delta(\Delta k_z')$$

with

$$m = a(\Delta k_{x'}^2 + \Delta k_{y'}^2)^{1/2} \quad , \tag{30}$$

where J_1 is the Bessel function of first order.

If there is no correlation between domains, the total scattered intensity is the sum of the intensity scattered by each domain, which is $4P_s^2|f(\Delta\vec{k})|^2$. In this summation process, as the radii a_i of the cylinders have a certain distribution, the oscillations of the Bessel function are lost and only the mean variation remains. As $J_1(m) \sim m^{-1/2}$ for large m, the asymptotic behavior for large Δk is proportional to $\sum_i a_i/(\Delta k)^3$, so the intensity for large scattering angles is proportional to the cylinder area.

A similar result can be obtained for cylindric domains with an elliptic cross section of length $2a$ along $0X'$ and $2va$ along $0Y'$. This is deduced by an affinity of ratio v from a circle, and its Fourier transform is

$$f(\Delta k) = \int_{\text{cylinders}} e^{i\Delta\vec{k}\cdot\vec{r}}\, d^3r = 4\pi^2 v a^2 [J_1(m)/m]\,\delta(\Delta k_{Z'})$$

with

$$m = |\Delta\vec{k}|\, a(1 + v^2\tan^2\theta)^{1/2}\cos\theta \quad , \tag{31}$$

where $\theta = (\vec{k}, 0\vec{X}')$.

If we suppose that there is no correlation between domains we only sum the intensity of individual domains. For ellipses of the same ratio v, constant intensity is obtained for m constant which gives an equi-intensity curve which is an ellipse of parameter v with its long axis perpendicular to the long axis of the domains' cross sections. As for circular cylinders, the asymptotic variation is in Δk^{-3}. The assumption of no correlation between domains is not very reliable particularly when there are many domains. So one can expect interference effects between domains, mainly for small $\Delta\vec{k}$. For greater $\Delta\vec{k}$ the interference effects between domains decrease, because then the intensity depends upon the variation of the correlation function $C(\vec{u})$ for small $\vec{u}$ which depends mainly on the form of domain surfaces. Then one can show that for cylinders the asymptotic variation for large Δk is always in Δk^{-3} (see the Appendix).

E. General Three-Dimensional Case

If the polarization depends on the three components of the spatial variable, we have a real problem in three-dimensional space, and there is scattered light in all directions. If there are no correlations between domains, we obtain results closely resembling those of small-angle x-ray scattering.[8] One cannot say much in the general case about the domain's correlation, and one must use appropriate models in each case. Only for the large scattering vector $\Delta\vec{k}$ do interference effects generally disappear and, as is shown in the Appendix, the asymptotic variation of the intensity is of the form $|\Delta\vec{k}|^{-4}$.

In studying all of the angular variation of SHS by ferroelectric domains, one can obtain, by Fourier inversion, the correlation function of the polarization. But if this inversion is not performed, one only gets some information on a particular point of the domain structure. To get a real picture of domains it would be necessary to preserve the information which is contained in the phase of scattered light waves by an appropriate experiment.

III. EXPERIMENTAL RESULTS ON TGS

We have previously reported the observation of SHS in TGS.[3,4] Here we present some new results

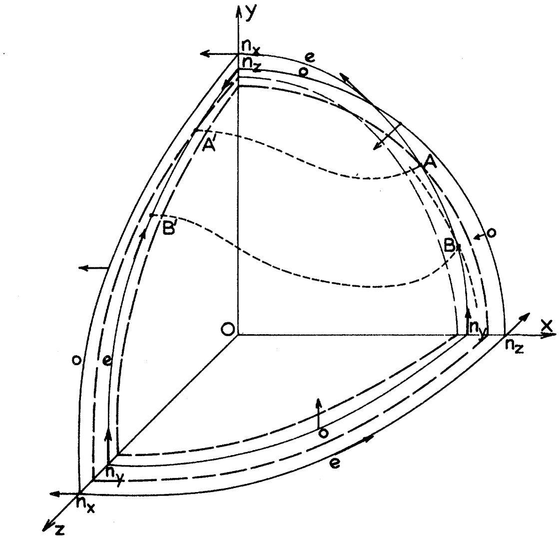

FIG. 1. Index surfaces of biaxial TGS for fundamental (6943 Å, broken line) and second-harmonic (3472 Å, full line) intensities. Dashed lines indicates phase-matching directions. Arrows show the polarization directions of ordinary (*o*) and extraordinary (*e*) light in principal planes.

on the influence of domain shapes on this effect at room temperature. Temperature dependence and phenomena near the Curie temperature were published elsewhere.[13]

A. SH Scattering in TGS

First we recall some properties of TGS[14]: It is an optically biaxial crystal with ferroelectric properties below the Curie temperature ($T_C = 49\,°\mathrm{C}$). The domains are cylinders parallel to the ferroelectric axis so we are dealing with the case of Sec. IID, and scattering vectors $\Delta\vec{k}$ are perpendicular to the ferroelectric axis. We choose an orthogonal reference frame with $0Y$ along the ferroelectric axis (also, the rotation axis is of order 2, which is the only symmetry element of the point group in the ferroelectric phase) and with $0X$ in the optic plane. The refractive index surface for fundamental (ruby laser light with wavelength 6943 Å) and SH (3472 Å) intensities are shown in Fig. 1. There are two kinds of phase matching, A and B, with

$$A:\ \vec{k}_{2e} = 2\vec{k}_{1o}\ ,$$

$$B:\ \vec{k}_{2e} = \vec{k}_{1o} + \vec{k}_{1e}\ ,$$

with subscripts 1 and 2 referring to fundamental and SH intensities, and o and e to ordinary and extraordinary polarization. One can see in Fig. 1 that there are two phase-matching directions A and B in the optic plane ($X0Y$) and two others, A' and B', in the other principal plane ($Y0Z$). The angles of these directions with the polar axis are given in Table I (with an uncertainty of about ±0.5°). These values were obtained with the experimental apparatus described before[4] in which the crystal is immersed in paraffin oil. The internal angles of the ordinary fundamental beams with $0Y$ were calculated using index values deduced from SH measurement as explained in Ref. 4. For comparison we also show the phase-matching angles given previously by Smith.[15] These are in fair agreement for A and B, but differ much for B' (called D by Smith); A' was not previously observed.

One must also note that θ_B and $\theta_{B'}$ are not characteristic of the crystal, but they depend on the angle of the surface normal to $0Y$. Indeed, these angles depend on the sum $\vec{k}_{1e} + \vec{k}_{1o}$ which depends on the direction of surface normal. In particular, the calculation of θ_B shows that there is no phase matching for a Y cut. Phase matching B is only possible when the angle of the surface normal to $0Y$ is great enough, which was the case for the experimentally obtained results.

All of the following results were obtained in plane-parallel slabs of about 2×10×10 mm perpendicular to the $0Y$ axis. The laser beam was incident either in the optic plane ($X0Y$) or in the perpendicular plane ($Y0Z$) where one has ordinary and extraordinary light. The polarization of light is then either parallel or perpendicular to the incidence plane. The incidence angle θ can be varied by rotating the crystal around a vertical axis ($0Z$ for light incident in the optic plane, $0X$ for light incident in $Y0Z$ plane).

We have shown previously that when the laser beam is in the optic plane there are five scattered lines labeled A to F. The existence of scattered lines is also observed when the incidence plane is $Y0Z$. The scattering angles of three lines A', B', and C' are plotted in Fig. 2 as a function of the incidence angle. All these lines have extraordinary polarization. In the $Y0Z$ plane we were not able to see the two ordinary lines which must exist, because their intensity was too small.

TABLE I. Angles of phase-matching directions, A and B in the ($X0Y$) plane and A' and B' in the ($Y0Z$) plane, with the polar axis.

Incidence plane	$Y0X$ (Optical plane)		$Y0Z$	
Phase matching	A	B	A′	B′
Angle of sample normal with OY	0	28.5°	0	0
Experimental external incidence angle	52°	37.5°	16.6°	44.5°
Calculated internal angle (from OY)	48.6°	63.8°	15.4°	40.6°
Results from Ref. 15	48.8°	64.5°	Not observed	32°

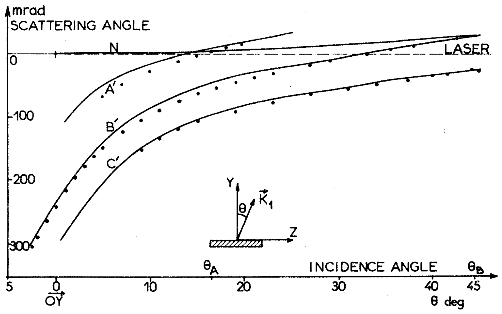

FIG. 2. Angular positions in air of scattered SH lines as a function of incidence angle in the plane YOZ perpendicular to the optic plane. N is the normal peak; A', B', and C' are scattered lines. Solid line: calculated values. Dots: experimental points.

One observes an analogous scattering pattern for negative incidence angles, with scattering angles opposite to the previous one. So on the plot of scattering angle versus incidence angle the origin is a center of symmetry. One can see in Fig. 2 that the B' line can be observed for value of the incidence angle on the two sides of the ferroelectric axis. So when the laser beam is near $0Y$ one can observe SH light scattered simultaneously on two sides of the normal. The propagation of different light waves in the crystal in this case is pictured in Fig. 3. There are two refracted fundamental beams, one ordinary and one extraordinary, which produce three nonlinear polarization waves with wave vectors $\vec{K}_{oo}, \vec{K}_{oe}, \vec{K}_{ee}$. The homogeneous SH contribution goes out into direction N. The scattering vectors $\Delta\vec{k}$ are contained in planes perpendicular to $0Y$ and pass by the extremities of vectors $\vec{K}$. These planes cut the SH index surfaces along nearly circular curves centered around $0Y$, giving the directions of SH waves inside the crystal. The external directions are obtained by Snell laws. So in the $Y0Z$ plane one obtains external SH waves in directions A' to F' near the laser direction and also in directions A'' to F'' on the other side of the ferroelectric axis, which can be considered as SH waves reflected on domains. The intensity of this line depends on laser-beam polarization and on the form of the nonlinear tensor. For example, for $\theta = 0$ the nonlinear polarization is along $0\vec{Y}$, so no SH waves are observed in the homogeneous contribution N, which is then in the $0Y$ direction. But SH waves from a nonlinear polarization along $0Y$ can be observed in scattering directions which make an angle greater than 0.2 rad with $0Y$. One can expect to see scattered SH waves all along a closed curve around $0Y$, but the intensity is large enough only for $\Delta\vec{k}$ near the $Y0Z$ plane (this is related to the anisotropy of domain cross sections as explained below). Thus, we only observe SH waves near B' and B'', the intensity of the other lines being far too small. One can follow the B' and B'' lines to 0.3 rad from the laser beam which corresponds to a coherence length of 1 μ. For greater $\Delta\vec{k}$ the intensity is too small to be observed with our apparatus.

The intensity variations of the normal peak and of several scattered lines as a function of incidence angle are given in Figs. 4 and 5 when the incidence plane is $Y0X$ and $Y0Z$. These curves were obtained on crystals which have remained for a long time at room temperature. The intensity peaks correspond to phase-matching directions. The direction $\theta = 0$ corresponding to the ferroelectric axis is marked by a sharp dip in Fig. 4. This dip is not observed in Fig. 5, due to small misalignment of the surface normal. The form of these intensity curves varies very much from one crystal to another, and also depends on the thermal treatment of the crystal.

B. Effect of Anisotropy of Domain Cross Sections

A limited length of domains along $0Y$ would produce scattering with $\Delta\vec{k}$ parallel to $0Y$. We have

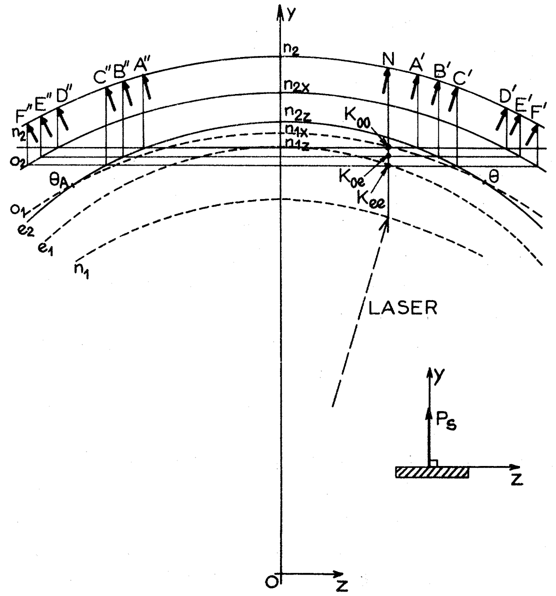

FIG. 3. Propagation of light waves for a laser beam incident near the ferroelectric axis. The sections of index surfaces by the YOZ plane are drawn with a dashed line for the fundamental intensity and a full line for the intensity SH; n_1 and n_2 correspond to the external medium and K_{oo}, K_{oe}, and K_{ee} are the extremities of the wave vectors of nonlinear polarization waves. N is the direction of the homogeneous waves. A' to F' are the directions of scattered lines near the laser beam; A'' to F'' are the directions of scattered lines on the other side of the ferroelectric axis.

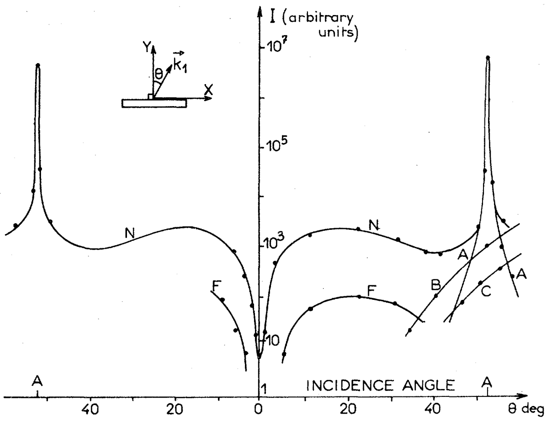

FIG. 4. Variation of SH intensity I (in arbitrary units) as a function of incidence angle for a laser beam in the optic plane $Y0X$. N is the normal contribution; A, B, C, and F are scattered lines.

never observed a transversal width of scattered lines greater than that due to the beam divergence (5 mrad). So the hypothesis of long domains along $0Y$ seems quite good.

It is also known, however, that TGS domains have a cross section elongated in a direction parallel to the optic plane.[16] The magnitude of this elongation varies from one crystal to the other, depending mainly on the impurity concentrations. If we suppose that domain cross sections are ellipses, with the same direction but with uncorrelated positions, from Sec. II the scattering curves would be anisotropic. For a given modulus of $\Delta\vec{k}$ one expects a greater intensity for $\Delta\vec{k}$ perpendicular to the optic plane than for $\Delta\vec{k}$ parallel to it. This effect is indeed observed as is shown in Fig. 6.

The two upper curves are obtained on a Y-cut crystal, with the optic plane $X0Y$ as incidence plane, near phase matching A. The intensity of a SH wave is plotted as a function of the modulus of $\Delta\vec{k}$ for given directions. The curve $\Delta\vec{k}_{\parallel}$ is obtained with $\Delta\vec{k}$ in the optic plane, parallel to the greatest domain dimension in rotating the crystal from an incidence angle of $\theta = 52°$ to $\theta = 44°$ to vary the modulus of $\Delta\vec{k}$. The curve $\Delta\vec{k}_{\perp}$ is obtained at $\theta = 52°$ (phase matching A) and in measuring the intensity along the scattered A line corresponding to a $\Delta\vec{k}$ nearly perpendicular to the incidence plane. With the $X0Y$ plane as incidence plane the scattered lines are quite well marked and extend relatively far from the incidence plane. The two lower curves are obtained with the incidence plane in $Y0Z$ near phase matching B'. $\Delta\vec{k}$ is now contained in the incidence plane and the corresponding curve was obtained in changing the incidence angle θ from 44.5° to 17.5°. For this geometry the scattered lines are rather sharp and decrease quickly when $\Delta\vec{k}$ goes out of the incidence plane; thus it was difficult to obtain directly the intensity variation along $\Delta\vec{k}$ because this intensity is screened by the far greater intensity of the phase-matching peak. It was necessary to use several orientations of the crystal near the phase-matching angle and to interpolate

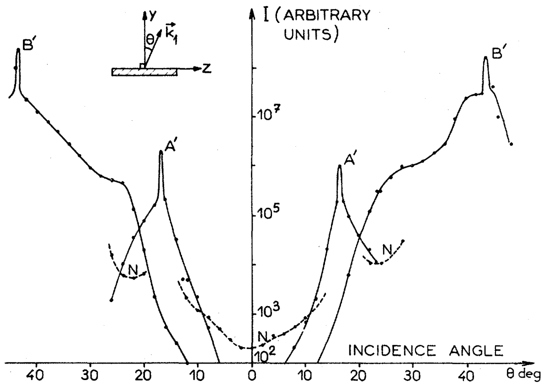

FIG. 5. Variation of SH intensity I as a function of incidence angle for a laser beam in the $Y0Z$ plane. N is the normal contribution. A' and B' are scattered lines. (N cannot be observed in the neighborhood of phase-matching angles because its intensity is smaller than that of A' or B'.)

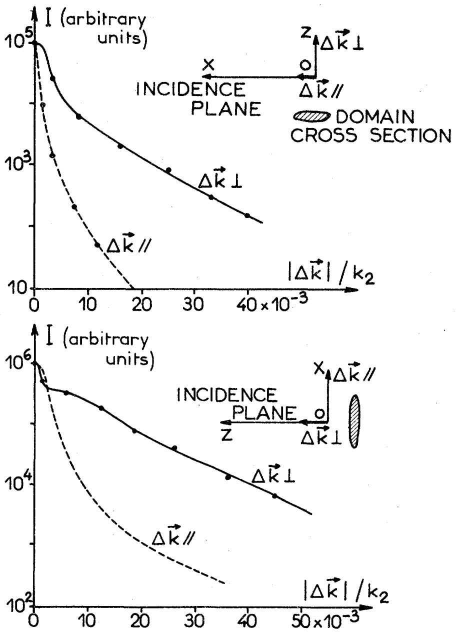

FIG. 6. Variation of intensity as a function of the modulus of $\Delta\vec{k}$ for $\Delta\vec{k}$ perpendicular and parallel to the great dimension of domains. Upper curves: incidence plane in the optic plane; lower curves: incidence plane perpendicular to the optic plane.

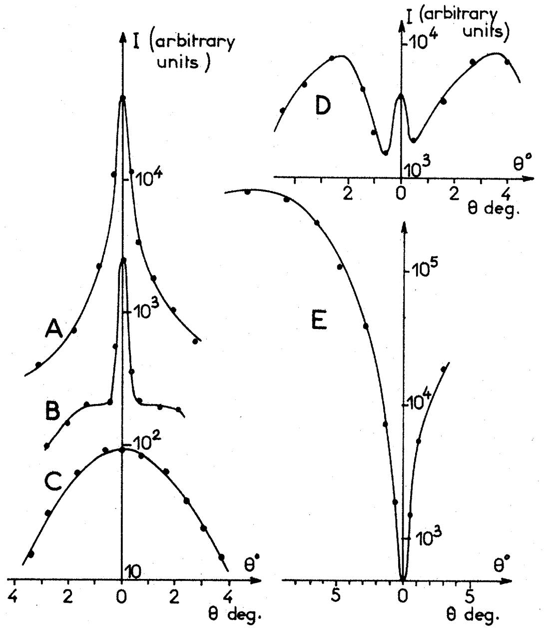

FIG. 7. Variation of SH intensity as a function of incidence angle near the phase-matching direction B' in the YOZ plane for various domain structure (see text). The curves A, B, and C have been shifted arbitrarily in the vertical direction.

this curve. But nevertheless, the general result appears clearly, for a given magnitude of $\Delta\vec{k}$ the intensity is greater for $\Delta\vec{k}$ perpendicular to the great domain dimension than for $\Delta\vec{k}$ parallel to it. For an elliptic cylinder of axes lengths a and b, equal intensities are obtained for

$$\Delta k_a a = \Delta k_b b \ .$$

As one sees in Fig. 6 that equal intensities are obtained for $\Delta k_\perp \sim 5\,\Delta k_\parallel$, one can deduce that the great dimension of cross sections is about five times greater than the small one. So the most intense SHS is observed for a $\Delta\vec{k}$ perpendicular to the optic plane. When the optic plane is the incidence plane there are broad scattered lines. When the incidence plane is YOZ, perpendicular to the optic plane, the scattered line is much narrower, with a sharp maximum. It is then easy to follow the intensity of this maximum as a function of the modulus of $\Delta\vec{k}$ to get the information about domain structure.

C. Effects of Thermal Treatments

As we have shown in Sec. II, the phase-matching intensity depends upon the mean polarization of the crystal, while the scattered intensity depends upon the number and the magnitude of domains. The shape of the phase-matching peak is very sensitive to the crystal state. Several typical shapes of the intensity variation as a function of the incidence angle near the phase-matching direction B' in the YOZ plane are plotted in Fig. 7. (Similar variations were previously observed by Sonin and Suvorov.[17])

Curve A corresponds to a nearly single domain crystal; it has a well-defined sharp peak, which looked like the curve $I = |(\sin\frac{1}{2}\Delta kl)/\Delta k|^2$. The foot of this peak is widened by the presence of domains. This curve is typical of crystals which have remained a long time at room temperature: There is little scattering, which shows that there are few domains, and there is a big peak which shows that the crystal is polarized in one sense. After heating a short time above the Curie temperature T_c and slow cooling (about 1 h) to room temperature, a curve such as B is obtained. One observes a peak, but now the bottom of the curve is very wide and domain scattering is quite intense. When the crystal is heated longer above T_c (for example, 12 h) one obtains intensity curves C or D, where the phase-matching peak has disappeared, and sometimes there is a dip in the curve in the phase-matching direction, showing that there is no longer a residual polarization. If the crystal has a mean polarization which is null, one gets a curve E where now there is a downward "peak" just in the phase-matching direction. The maxima

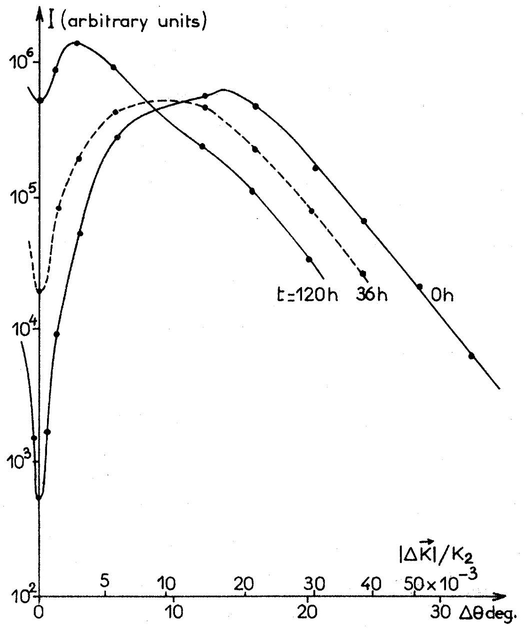

FIG. 8. Evolution with time of the scattered intensity. The variation of intensity I as a function of the modulus of the scattering vector $\Delta\vec{k}$ is plotted at three time intervals after a rapid cooling from the paraelectric phase to room temperature. $|\Delta\vec{k}|$ is measured relative to the length of $\vec{k}_2$; wave vectors of SH light are in a vacuum.

of the intensity correspond to $\Delta k = \pi/a$, where a is of the order of magnitude of domain widths.

Often these curves change with time, following the evolution of domain structure. For example, Fig. 8 shows the variation with time of the depolarized crystal of curve E of Fig. 7. One sees that the $\Delta k = 0$ intensity increases, showing a partial repolarization of the sample. At the same time, there is a shift of the intensity maximum towards smaller Δk, indicating an increase in domain width from about 10 to 70 μ, which was previously observed in TGS by etching.[18] It is possible to study the variation of domain structure by observing the variation of SHG near a phase-matching direction.

IV. CONCLUSION

In this paper we have shown that the study of SHS by ferroelectric domains can be used to obtain information on domain structures. Very different patterns of scattered light are obtained for plane-parallel cylindrical- or arbitrary-shaped domains. An example of the use of this technique has been presented here, in the case of cylindrical domains of TGS, where we have observed the effects of domains on the SH intensity. One can hope that a systematic study of SHG can give more quantitative information on domain structure and its evolution under various external conditions (temperature, applied electric field, etc.).

ACKNOWLEDGMENTS

The author wishes to thank Professor J. Lajzerowicz and M. Vallade for many fruitful discussions and also the latter for his assistance in the experimental work.

APPENDIX

We will calculate the asymptotic variation of the intensity scattered by one domain for a large scattering vector in one, two, and three dimensions. This result can easily be deduced from Erdéleyi's theorem[19,20] which gives the asymptotic behavior of the Fourier transform $F(k)$ of a function $f(x)$, which we will use in two particular cases:

$$F(k) = \int_a^b f(x)\, e^{ikx}\, dx \qquad \text{(A1)}$$

if $f(x)$ is one-time continuously differentiable;

$$F(x) = i\,\frac{f(b)\,e^{ikb} - f(a)e^{ika}}{k} + \frac{f'(b)\,e^{ikb} - f'(a)\,e^{ika}}{k^2} + O(k^{-2}) \qquad \text{(A2)}$$

[where $O(k^{-2})$ indicates a term which tends to zero faster than k^{-2}]: If $f(x)$ is regular between a and b but singular at $x = a$ and $x = b$. Then $f(x) \sim (x - a)^{1/2}$ when $x \to a$ and $f(x) \sim (x - b)^{1/2}$ when $x \to b$ and, therefore, $F(k) \sim k^{-3/2}$ when $k \to \infty$.

In one dimension the form factor of a domain is given by $f(x) = 1$ for x inside the domain and $f(x) = 0$ for x outside. So from (A2), $F(k) \sim k^{-1}$, and the intensity proportional to $|F(k)|^2$ decreases like k^{-2}.

In two dimensions a domain is limited by curve C and its form factor is $f(x, y) = 1$ if the point (x, y) is inside C and $f(x, y) = 0$ if (x, y) is outside. If we choose an axis $0X$ parallel to the direction of vector $\vec{k}$, then

$$F(k) = \int\int_{-\infty}^{+\infty} f(x, y)\, e^{ikx}\, dx\, dy = \int_{-\infty}^{+\infty} D(x)\, e^{ikx}\, dx \, , \qquad \text{(A3)}$$

where $D(x)$ is the length of the straight line of abscissa x contained in C. In general, $D(x)$ is a regular function except when curve C has a tangent perpendicular to $0X$. If a and b are the abscissa of such points, without other singularities between them, we can apply the second case of Erdéleyi's theorem. To calculate the singular variation of $D(x)$ near $x = a$, for example, we replace curve C by a circle with the same radius of curvature as C and make a change of variable $x = a + u$.

Then the equation of this circle of radius R is

$$y^2 + (R - u)^2 = R^2 \, ,$$
$$D(u) = 2y(u) \simeq 2(2Ru)^{1/2} \, . \qquad \text{(A4)}$$

The asymptotic variation of $F(k)$ is in $k^{-3/2}$ and that of $|F(k)|^2$ is in k^{-3}. If points with tangents perpendicular to $0X$ have a random distribution, one has only to sum their respective intensity to get the total scattered intensity.

For a three-dimensional volume V with a form factor $f(x, y, z)$ limited by a surface Σ we also take an axis parallel to the wave vector $\vec{k}$,

$$F(k) = \int\int\int_V f(x, y, z)\, e^{ikx}\, dx\, dy\, dz = \int_{-\infty}^{+\infty} S(x)\, e^{ikx}\, dx \, , \qquad \text{(A5)}$$

where $S(x)$ is the surface of the section of V by a plane of abscissa x. As in two dimensions, for a regular surface Σ we must calculate the variation of $S(x)$ near the points with a tangent plane perpendicular to $0X$. To do this we write the equation of Σ in a rectangular reference frame, with its origin at a point A of a tangent plane perpendicular to $0X$ and retain only terms to second order. Σ is then approximated by a quadric, which is, in general, an ellipsoid, and its section by a plane is an ellipse. At point A, the ellipsoid has two principal radii of curvature R_1 and R_2 in two perpendicular planes. The lengths of the two axis of the ellipse are

$$a = (2R_1 x)^{1/2}, \quad b = (2R_2 x)^{1/2} ,$$

$$S(x) = \pi ab = 2\pi(R_1 R_2)^{1/2} x .$$

Then $F(k)$ for large k varies as k^{-2} and $|F(k)|^2$ as k^{-4}. For other kinds of singular points the asymptotic dependence can change, consequently, the scattered intensity for large k in one, two, and three dimensions varies, respectively, as k^{-2}, k^{-3}, and k^{-4} for contours and surfaces without singularities.

---

[1] N. Bloembergen, *Nonlinear Optics* (Benjamin, New York, 1965).

[2] I. Freund, Phys. Rev. Letters 21, 1404 (1968).

[3] G. Dolino, J. Lajzerowicz, and M. Vallade, Solid State Commun. 7, 1005 (1969).

[4] G. Dolino, J. Lajzerowicz, and M. Vallade, Phys. Rev. B 2, 2194 (1970).

[5] R. C. Miller, Phys. Rev. 134, A1313 (1964).

[6] D. A. Kleinman, Phys. Rev. 128, 1761 (1962).

[7] D. A. Kleinman, A. Ashkin, and G. D. Boyd, Phys. Rev. 145, 338 (1966).

[8] A. Guinier and G. Fournet, *Small Angle Scattering of X-Rays* (Wiley, New York, 1955).

[9] L. Schwartz, *Méthodes Mathématiques pour les Sciences Physiques* (Herman & Cie, Paris, 1965).

[10] E. Fatuzzo and W. J. Merz, *Ferroelectricity* (North-Holland, Amsterdam, 1967).

[11] H. Vogt, H. Happ, and H. F. Hafele, Phys. Status Solidi 1a, 439 (1970).

[12] A. Blanc-Lapierre and R. Fortet, *Théorie des fonctions Aléatoires* (Masson, Paris, 1953), p. 189.

[13] G. Dolino, J. Lajzerowicz, and M. Vallade, *International Conference on Light Scattering in Solids* (Flammarion, Paris, 1971), p. 439.

[14] F. Jona and G. Shirance, *Ferroelectrical Crystals* (McMillan, New York, 1962).

[15] A. W. Smith, Appl. Opt. 3, 147 (1964).

[16] A. G. Chynoweth and J. L. Abel, J. Appl. Phys. 30, 1073 (1959).

[17] A. S. Sonin and V. S. Suvorov, Fiz. Tverd. Tela 10, 1031 (1968) [Sov. Phys. Solid State 10, 814 (1968)].

[18] F. Moravets and V. P. Konstantinova, Kristallogr. 13, 284 (1968) [Sov. Phys. Crist. 13, 221 (1968)].

[19] A. Erdeleyi, J. Soc. Ind. Appl. Math 3, 17 (1955).

[20] A. Papoulis, *Systems and Transforms with Applications to Optics* (McGraw-Hill, New York, 1968).

PHYSICAL REVIEW B VOLUME 6, NUMBER 10 15 NOVEMBER 1972

Generalized Random-Walk Model for Singlet-Exciton Energy Transfer*

Zoltán G. Soos† and Richard C. Powell‡
Sandia Laboratories, Albuquerque, New Mexico 87115

(Received 23 July 1971; revised manuscript received 2 June 1972)

The usual model for singlet-exciton motion and trapping in molecular crystals is generalized to arbitrary finite trapping regions about each activator and to more than nearest-neighbor steps by the random walker. The properties of extended trapping regions, which simulate activator-induced host traps, are obtained rigorously by applying general results for three-dimensional random walks. The capacity $C(A)$ of the extended trapping region is shown, by explicit calculations for a simple cubic lattice, to depend on the size and shape of the trapping region and on the anisotropy and step distribution of the random walker. The capacity controls the competition between singlet-exciton absorption (trapping and subsequent trap fluorescence) and emission (host fluorescence) observed in doped organic crystals. The model accounts qualitatively for the "anomalous" time dependence of the energy-transfer rate in tetracene-doped anthracene and in anthracene- or tetracene-doped naphthalene. The model also accounts for the reported variations in the apparent exciton hopping time, which provide strong evidence for the hypothesis of extended trapping regions.

I. INTRODUCTION

Both exciton diffusion[1,2] and long-range resonant transfer[3,4] (LRRT) describe the motion of singlet excitations in molecular crystals. LRRT has been thoroughly documented for energy transfer between immobile excitations on impurities embedded in the crystal. Simpson[5] demonstrated singlet-exciton diffusion in anthracene and Trlifaj[2] related theoretically the diffusion constant to the efficient LRRT between adjacent host sites. In the following, we reserve "diffusion" for nearest-neighbor random walking by whatever mechanism of the singlet excitation.

Powell and Kepler[6–11] (PK) recently observed the time evolution of both sensitizer (host) and activator (trap) fluorescence in doped organic crystals. Singlet-exciton motion in either crystalline anthracene or naphthalene, the two hosts studied by PK, is generally thought to be diffusional at room temperature, where the shallow host traps which are observed at low temperature are thermally detrapped. The PK data nevertheless decisively rule out the usual formulation of exciton